Acta Pharmacologica Sinica (2015) 36: 1426–1436
 1671-4083/15
www.nature.com/aps

Original Article

Carvacrol protects neuroblastoma SH-SY5Y cells against Fe^{2+}-induced apoptosis by suppressing activation of MAPK/JNK-NF-κB signaling pathway

Zhen-wen CUI[1, #], Zheng-xing XIE[1, #], Bao-feng WANG[1], Zhi-hong ZHONG[1], Xiao-yan CHEN[3], Yu-hao SUN[1], Qing-fang SUN[1], Guo-yuan YANG[2, 3], Liu-guan BIAN[1, *]

[1]*Department of Neurosurgery, Ruijin Hospital, Shanghai Jiao Tong University School of Medicine, Shanghai 200025, China;* [2]*Department of Neurology, Ruijin Hospital, Shanghai Jiao Tong University School of Medicine, Shanghai 200025, China;* [3]*Neuroscience and Neuroengineering Research Center, Med-X Research Institute, Shanghai Jiao Tong University, Shanghai 200030, China*

Aim: Carvacrol (2-methyl-5-isopropylphenol), a phenolic monoterpene in the essential oils of the genera *Origanum* and *Thymus*, has been shown to exert a variety of therapeutic effects. Here we examined whether carvacrol protected neuroblastoma SH-SY5Y cells against Fe^{2+}-induced apoptosis and explored the underlying mechanisms.
Methods: Neuroblastoma SH-SY5Y cells were incubated with Fe^{2+} for 24 h, and the cell viability was assessed with CCK-8 assay. TUNEL assay and flow cytometric analysis were performed to evaluate cell apoptosis. The mRNA levels of pro-inflammatory cytokines and NF-κB p65 were determined using qPCR. The expression of relevant proteins was determined using Western blot analysis or immunofluorescence staining.
Results: Treatment of SH-SY5Y cells with Fe^{2+} (50–200 μmol/L) dose-dependently decreased the cell viability, which was significantly attenuated by pretreatment with carvacrol (164 and 333 μmol/L). Treatment with Fe^{2+} increased the Bax level and caspase-3 activity, and decreased the Bcl-2 level, resulting in cell apoptosis. Furthermore, treatment with Fe^{2+} significantly increased the gene expression of IL-1β, IL-6 and TNF-α, and induced the nuclear translocation of NF-κB. Treatment with Fe^{2+} also significantly increased the phosphorylation of p38, ERK, JNK and IKK in the cells. Pretreatment with carvacrol significantly inhibited Fe^{2+}-induced activation of NF-κB, expression of the pro-inflammatory cytokines, and cell apoptosis. Moreover, pretreatment with carvacrol inhibited Fe^{2+}-induced phosphorylation of JNK and IKK, but not p38 and ERK in the cells.
Conclusion: Carvacrol protects neuroblastoma SH-SY5Y cells against Fe^{2+}-induced apoptosis, which may result from suppressing the MAPK/JNK-NF-κB signaling pathways.

Keywords: carvacrol; Fe^{2+}; neurotoxicity; MAPK; JNK; NF-κB; pro-inflammatory cytokines; apoptosis

Acta Pharmacologica Sinica (2015) 36: 1426–1436; doi: 10.1038/aps.2015.90; published online 23 Nov 2015

Introduction

Iron-mediated free radical damage, which is associated with cerebrovascular disease, is thought to be involved in neuronal cell injury in acute brain pathological states including ischemia and intracerebral hemorrhage and in the neuropathology of several degenerative diseases, such as Alzheimer's disease (AD) and Parkinson disease (PD)[1-4]. Iron, which is released from heme after hemoglobin breakdown, accumulates in the parenchyma. This ferrous iron has been associated with brain edema and cell death. Previous studies have proved that an increase in extracellular free Fe^{2+} (even as low as 1μmol/L) effectively promotes Fe^{2+} entry and intracellular iron load[5]. The toxicity of iron overload is known to result from a reaction with oxygen and to generate massive oxidative damage involving lipid peroxidation and mitochondrial dysfunction via Fenton reaction[6]. In addition, an Fe^{2+}-induced increase in the formation of reactive oxygen species (ROS) can also activate diverse signaling pathways and result in a variety of responses, including inflammatory responses[7, 8]. Therefore, the toxicity of iron overload is often associated with inflammation, which is involved in pathogenic effects, including damage to neurons[9]. It has been reported that the production of proinflammatory cytokines, such as IL-1β, IL-6 and TNF-α is upregulated following ischemia and intracerebral hemorrhage, which results in neuroinflammation[10, 11]. These cytokines are key mediators of

# These authors contributed equally to this work.
* To whom correspondence should be addressed.
E-mail rj1111@yahoo.com
Received 2015-05-03 Accepted 2015-08-26

inflammatory responses, and their overexpression can further activate downstream apoptotic signaling pathways in neurons, which ultimately results in neuronal death[12].

NF-κB is a ubiquitous nuclear transcription factor that plays a critical role in the regulation of many genes that encode for mediators of immune and inflammatory responses[13]. There is evidence showing that NF-κB levels are increased in cells surrounding intracerebral hemorrhage[14] and that NF-κB-dimers are translocated from the cytoplasm into nucleus in Fe^{2+}-activated microglia *in vitro*[15]. In addition, the activation of NF-κB has also been demonstrated in both neurons and glial cells in many neurological diseases[16]. Inhibition of NF-κB activity has been shown to protect neuronal cells against iron-induced neuronal apoptosis[15, 17, 18]. Furthermore, it has been shown that the activation of NF-κB is mediated by a wide variety of upstream signals, including the MAPKs[15, 18, 19], which comprise three protein kinases: JNK, p38, and ERK. The MAPKs are sensitive to stimulators that cause oxidative stress, including metal neurotoxicity[20]. It is also involved in cellular responses to proinflammatory and other stress signals. Emerging evidence has demonstrated that MAPKs play a critical role in microglia-mediated neuronal death in neurodegenerative diseases and that the inhibition of MAPKs may protect dopaminergic neuron from apoptosis[15, 21].

Carvacrol (2-methyl-5-isopropylphenol), a phenolic monoterpene, is mainly found in the essential oils extracted from many plants belonging to the Lamiaceae family, such as the genera *Origanum* and *Thymus*. Carvacrol is generally considered to be a safe food additive and flavoring agent[22]. Recently, an increasing number of studies have focused on its therapeutic potential in different diseases. It has been reported that carvacrol has a wide range of protective properties, including anti-inflammatory, antioxidant, antimicrobial, antitumor, and anti-hepatotoxic activities[23-26]. For example, studies have reported that carvacrol has the ability to protect the liver and brain against ischemia/reperfusion (I/R) injury in *in vivo* studies[27-29]. Carvacrol also attenuated the impairment caused by acute myocardial infarction in rats via its antioxidative and anti-apoptotic properties[30]. Recently, some studies have demonstrated that carvacrol has anti-inflammatory properties and that the mechanisms involved in its pharmacological activities might be related to the modulation of several important molecular targets, including NF-κB, COX-2 and pro-inflammatory cytokines, such as IL-1β and TNF-α[31-34].

Based on data in previous studies, in this study, we aimed to explore the molecular mechanisms involved in Fe^{2+}-induced apoptosis in SH-SY5Y cells and to determine whether the activation of NF-κB and the expression of inflammation cytokines were involved in this process. Importantly, these experiments were designed to investigate whether carvacrol confers neuroprotective effects against Fe^{2+}-induced neuronal cell death and to determine the related signaling pathways.

Materials and methods

Materials

SH-SY5Y cells were acquired from the Cell Bank of the Shanghai Institute of Cell Biology and Biochemistry, Chinese Academy of Sciences (Shanghai, China). Carvacrol (Sigma-Aldrich, USA) was dissolved in dimethyl sulfoxide (DMSO), and the DMSO content in all treatment groups was 0.1%. BAY11-7082 (Beyotime, China), SB203580 (Santa Cruz Biotechnology, USA), U0126 (Santa Cruz Biotechnology, USA) and SP600125 (Santa Cruz Biotechnology, USA) were used as NF-κB and MAPK inhibitors at a concentration of 10 μmol/L. $FeCL_2{\cdot}4H_2O$ was acquired from Sinopharm Chemical Reagents (Shanghai, China). The anti-NF-κB/p65 and anti-p-IKKα/β antibodies were purchased from Santa Cruz Biotechnology (Santa Cruz, CA, USA). The antibodies against ERK, phospho-ERK, JNK, phospho-JNK, p38, phospho-p38, Bcl-2, Bax, cleaved caspase-3, and β-actin were purchased from Cell Signaling (Boston, USA).

Cell culture

Human SH-SY5Y dopaminergic neuroblastoma cells were cultured in Dulbecco's modified Eagle's medium (DMEM) containing 4.5 g/L glucose, 3.7 g/L sodium bicarbonate, 4 mmol/L glutamine, 10% fetal bovine serum, 100 units/mL penicillin, and 100 mg/mL streptomycin. Cells were maintained in a humidified cell culture incubator at 37 °C with 5% CO_2 atmosphere, as instructed by the manufacturer. For all experiments, cells were trypsinized and seeded at a density of 0.5 to 1.0×10^4 cells per cm^2 onto tissue culture-treated plastic ware.

Cell viability assay

SH-SY5Y cells were plated at a density of 1×10^4 cells per well in 96-well plates. All experiments were carried out 24 h after cells had been seeded. Cells were then incubated with different concentrations of Fe^{2+} for another 24 h. Some cells were incubated with carvacrol for 2 h prior to treatment with Fe^{2+} for another 24 h without a change in the culture medium. The control-cultured cells were incubated with culture medium for 24 h. Cell viability was determined using 2-(2-methoxy-4-nitrophenyl)-3-(4-nitrophenyl)-5-(2,4-disulfophenyl)-2*H*-tetrazolium and monosodium salt (WST-8) with a Cell Counting Kit-8 (CCK-8) assay (Beyotime Biotechnology, China) according to the manufacturer's instructions. Briefly, after treatment, 90 mL of cell suspension was incubated with 10 mL of WST-solution for 4 h at 37 °C in a 5% CO_2 atmosphere, and then the assay was stopped. The absorbance of the samples at a wavelength of 450 nm was measured using a microplate reader (BioTek, USA).

In situ cell death detection

To evaluate cell apoptosis, TdT-dUTP nick-end labeling (TUNEL) assays were performed using a one step *in situ* cell death detection kit (Roche, Germany) according to the manufacturer's instructions. Briefly, after the induction of apoptosis, cells were fixed with 4% paraformaldehyde in PBS (pH 7.4) for 1 h at room temperature, washed in PBS, and then incubated with 0.1% Triton X-100 for 2 min on ice. Later, the cells were incubated in TUNEL reaction mixture in a humidified atmosphere for 1 h at 37 °C in the dark. DAPI (1:5000, Invitrogen, USA) was used to label nuclei. TUNEL-positive cells

were imaged under a fluorescence microscope. Cells showing red fluorescence were considered apoptotic cells.

Flow cytometric analysis

Apoptosis was further determined by using Annexin V-FITC apoptosis kits (Beyotime, China), which detect cell surface changes that occur early in the apoptotic process. The assays were performed according to the manufacturer's instructions. Briefly, after treatment, 1×10^5 cells were washed twice with PBS and stained with 5 μL of Annexin V-FITC and 10 μL of PI in 195 μL of binding buffer for 15 min at room temperature in the dark. Then, the rates of apoptosis were analyzed in an Accuri C6 flow cytometer (Becton Dickinson) and determined using FlowJo software.

Total RNA extraction and relative quantitative real time-PCR analysis

Total RNA was extracted from cell cultures using TRIzol reagent (Invitrogen, USA). Extracts were treated with RNase-free DNase to remove any residual genomic DNA. Reverse transcription was performed using a Prime-Script RT reagent kit (TaKaRa Bio Inc, China). The oligonucleotide primers used to amplify the target genes were as follows: GADPH, 5′-AGCCACATCGCTCAGACAC-3′ (forward) and 5′-GCCCAATACGACCAAATCC-3′ (reverse); IL-1β, 5′-ATGGGATAACGAGGCTTATGTG-3′ (forward) and 5′-CAAGGCCACAGGTATTTTGTC-3′ (reverse); IL-6, 5′-ACTTGCCTGGTGAAAATCAT-3′ (forward) and 5′-CAGGAACTGGATCAGGACTT-3′ (reverse); TNF-α, 5′-TCAGCAAGGACAGCAGAGG-3′ (forward) and 5′-CAGTATGTGAGAGGAAGAGAACC-3′ (reverse); and NF-κB, 5′-TATTTCAACCACAGATGGCACT-3′ (forward) and 5′-AGCAAAGGCAATACATACACTT-3′ (reverse). GAPDH was used as a reference gene to calculate ΔCt. PCR amplification was performed using the following program: 95 °C for 40 s, 55 °C for 45 s, and 72 °C for 50 s. After 40 cycles, the relative levels of gene expression were quantified using SDS software (Applied Biosystems, Carlsbad, CA USA).

Extraction of nuclear and cytosolic fractions

The extraction and isolation of nuclear and cytoplasmic proteins were performed according to the manufacturer's instructions using a nuclear and cytoplasmic protein extraction kit (Beyotime, Jiangsu, China). Briefly, after treatment, cells were washed twice with PBS, scraped and collected by centrifugation at 1500×*g* for 5 min. Cell pellets were resuspended in 200 mL extraction buffer A and incubated for 15 min on ice. Afterwards, extraction buffer B was added, and samples were vortexed for 30 s at 4 °C. After centrifugation at 12000×*g* for 5 min at 4 °C, supernatants, which contained the cytosolic fractions, were removed and stored at -80 °C until analyzed by gel electrophoresis. Pellets, which contained the nuclei, were resuspended in 50 mL of nuclear extraction buffer, and nuclear proteins were extracted by shaking the samples for 30 min at 4 °C. Afterwards, samples were centrifuged at 12000×*g* for 5 min at 4 °C. The supernatants were removed and analyzed using gel electrophoresis. The validation of the method used to isolate the cytosolic and nuclear fractions (histone-H3 was used as a loading control for nuclear proteins, and β-actin wasused as the loading control for cytoplasm proteins) was checked using Western blot analysis.

Western blot analysis

Proteins were extracted from cell cultures after the treatments, and protein concentrations were determined by BCA assay (Pierce Biotechnology, USA). Equal amounts of proteins (30 μg) were loaded onto an 8% polyacrylamide gel for electrophoresis and then electrotransferred onto PVDF membranes. Blots were blocked with 5% non-fat milk and incubated with the appropriate primary antibodies at 4 °C overnight. After washing the blots 3 times, the membranes were incubated with HRP-anti-rabbit IgG for 1 h at room temperature. Protein signals were detected using an ECL chemiluminescence system (Pierce Biotechnology, USA). Densitometric analysis of bands was performed using ImageJ software (V1.40).

Immunofluorescence

The SH-SY5Y cells were seeded in a 24-well chamber slide and pretreated with 333 μmol/L carvacrol for 2 h before 200 μmol/L $Fe^{2+}$was added. After incubation for 2 h, the cells were fixed in cool methanol for 5 min and then treated with 0.3% Triton X-100 for 20 min, blocked in 10% bovine serum albumin for 30 min, and incubated overnight at 4 °C with primary anti-NF-κB p65 (1:100) antibodies. After being washed, the sections were incubated with secondary antibodies, Alexa Fluor 488 donkey anti-rabbit IgG (1:500, Invitrogen, USA), for 1 h. DAPI (1:5000, Invitrogen, USA) was used to label the nuclei. Fluorescence images were acquired using a confocal laser-scanning microscope.

Statistical analysis

All data are expressed as the mean±SD and were analyzed using SPSS version 18 software. Differences among groups were evaluated by one-way analysis of variance followed by Student–Newman–Keuls tests or two-way analysis of variance followed by Bonferroni *post hoc* tests. A *P*-value of <0.05 was considered statistically significant. Statistical results are reported in the figure legends.

Results

Effects of carvacrol on cell toxicity induced by exposure to Fe^{2+}

To investigate the toxicity of ferrous iron and carvacrol in SH-SY5Y cells and to determine the influence of carvacrol on Fe^{2+} toxicity in these cells, the SH-SY5Y cells were treated with 10, 50, 100, 200 or 300 μmol/L of Fe^{2+} and 33, 66, 164, 333, or 666 μmol/L of carvacrol for 24 h. CCK-8 assays were performed to assess cell viability. The viability of cells incubated with Fe^{2+} at 10, 50, 100, 200 and 300 μmol/L for 24 h was 93.2%±7.5%, 88.0%±2.0%, 79.0%±5.3%, 65.0%±2.5%, and 53.0%±2.2% of the control values, respectively (Figure 1A). The results showed that Fe^{2+} at 10–300 μmol/L gradually decreased cell viability, with significant decreases at 200 and 300 μmol/L of Fe^{2+}, compared to the untreated control cells. Fe^{2+} at 200 μmol/L was chosen for the following experiments. The presence of up to

333 μmol/L carvacrol did not affect the viability of SH-SY5Y cells (Figure 1B), suggesting that the carvacrol concentration used in this study was not cytotoxic. The decrease in viability of cells that was caused by 200 μmol/L of Fe^{2+} was significantly prevented by pretreatment with 164 and 333 μmol/L of carvacrol (Figure 1C). Likewise, as shown in Figure 1D, exposure to Fe^{2+}at 200 μmol/L caused clear morphological alterations that were typical of neuronal damage, while pretreatment with carvacrol for 2 h before Fe^{2+} exposure partially attenuated iron-induced cytotoxicity and cell damage.

Carvacrol inhibits Fe^{2+}-induced apoptotic cell death in SH-SY5Y cells

Because the intrinsic apoptotic pathway is mainly regulated by proteins that belong to the Bcl-2 and caspase families, changes in the expression of either pro-apoptotic or antiapoptotic Bcl-2 and caspase family members can affect the induction of apoptosis. To determine whether carvacrol acts by modulating the abundance of apoptotic proteins, the protein levels of Bax, Bcl-2 and caspase-3 were measured using Western blot analysis. SH-SY5Y cells were pretreated with carvacrol (333 μmol/L) and then exposed to Fe^{2+} for another 24 h. As shown in Figure 2A, exposure to Fe^{2+}at 200 μmol/L for 24 h significantly increased Bax expression and decreased Bcl-2 expression, while pretreatment with carvacrol inhibited the upregulation of Bax and the downregulation of Bcl-2. Consistent with these results, exposure to Fe^{2+} at 200 μmol/L for 24 h significantly increased cleaved caspase-3 protein levels compared to control conditions, indicating the involvement of caspase-3 in Fe^{2+}-induced cell death in SH-SY5Y cells (Figure 2B), whereas pretreatment with carvacrol (333 μmol/L) for 2 h significantly downregulated the elevated protein expression of cleaved caspase-3.

In addition, Fe^{2+}-induced apoptotic cell death was further confirmed by the detection of TUNEL-positive staining *in situ* and flow cytometric analysis. The results showed that Fe^{2+} significantly increased the number of apoptotic cells compared to untreated cells. Pretreatment with carvacrol (333 μmol/L) for 2 h prior to Fe^{2+} exposure, however, partially attenuated the increased proportion of apoptotic cells (Figure 2C and 2D). These results demonstrate that carvacrol effectively blocks Fe^{2+}-induced apoptotic cell death.

Carvacrol downregulates the expression of IL-1β, IL-6 and TNF-α in Fe^{2+}-stimulated SH-SY5Y cells

Proinflammatory cytokines, such as IL-1β, IL-6 and TNF-α, are thought to be involved in mediating neuroinflammation and inducing neuronal death in various neurodegenerative diseases. Therefore, we investigated the effect of Fe^{2+} on the expression of IL-1β, IL-6 and TNF-α. To detect its effect on the mRNA expression of proinflammatory factors using qPCR, we pretreated SH-SY5Y cells with carvacrol for 2 h and then exposed these cells to Fe^{2+} for 24 h. The results demonstrated that stimulation of SH-SY5Y cells with Fe^{2+} led to increases in the expression of IL-1β, IL-6 and TNF-α (Figure 3). However,

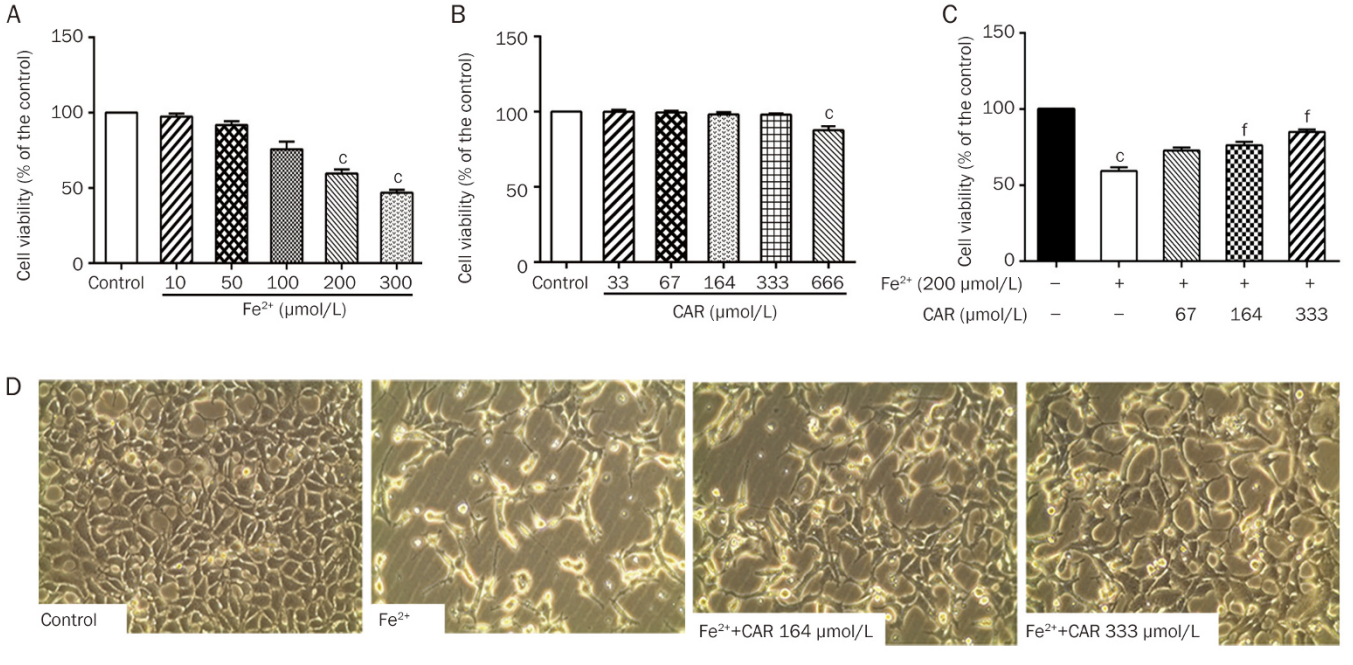

Figure 1. The protective effects of carvacrol against Fe^{2+}-induced cytotoxicity in SH-SY5Y cells. (A) SH-SY5Y cells were treated with different concentrations of Fe^{2+} (10, 50, 100, 200 or 300 μmol/L) for 24 h, and cell viability was estimated using CCK-8 assays. (B) SH-SY5Y cells were treated with different concentrations of carvacrol (33, 67, 164, 333 or 666 μmol/L) for 24 h. Cell viability was estimated using CCK-8 assays. (C) Cells were pretreated with 67, 164 or 333 μmol/L carvacrol for 2 h and then incubated with 200 μmol/L Fe^{2+} for 24 h. (D) Cells were pretreated with 164 or 333 μmol/L carvacrol for 2 h prior to treatment with Fe^{2+} (200 μmol/L) for 24 h, and then morphological changes were analyzed (200×). CAR, carvacrol. Mean±SD (n=3). ^{c}P<0.01 *vs* the untreated control; ^{f}P<0.01 *vs* the Fe^{2+}-treated group.

the production of these pro-inflammatory mediators was significantly inhibited by carvacrol. Furthermore, BAY11-7082 (10 μmol/L), an inhibitor of NF-κB, also significantly inhibited Fe^{2+}-induced IL-1β, IL-6 and TNF-α expression (Figure 3).

NF-κB expression in Fe^{2+}-treated SH-SY5Y cells

Previous studies have shown that NF-κB activation is necessary for the induction of proinflammatory mediators[13, 35]. Next, we wanted to investigate whether NF-κB was modu-

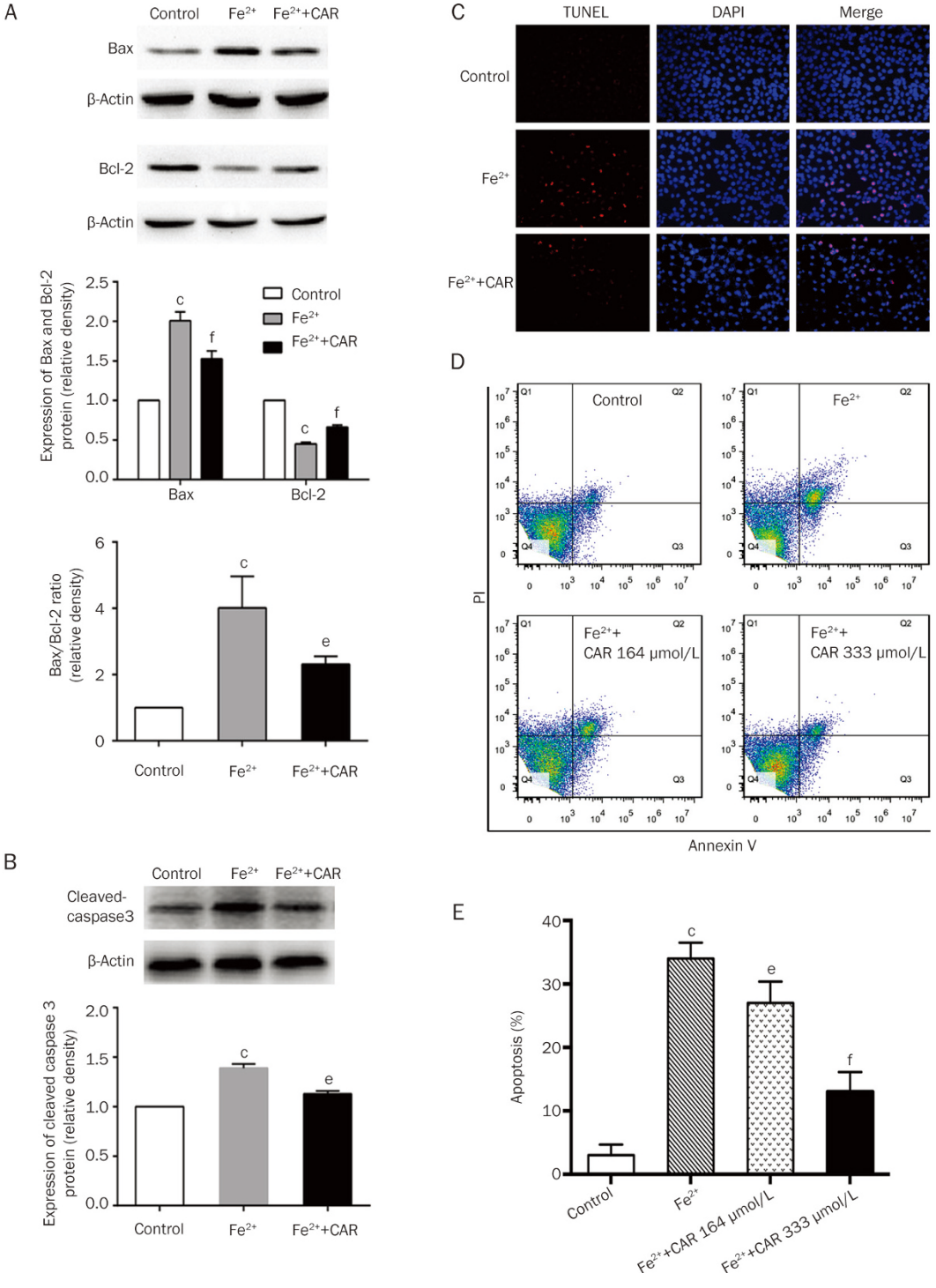

Figure 2. Carvacrol inhibits Fe^{2+}-induced apoptotic cell death in SH-SY5Y cells. Fe^{2+} (200 μmol/L, 24 h) caused a significant increase in the Bax/Bcl-2 ratio (A) and cleaved caspase-3 expression (B) in SH-SY5Y cells, which was significantly attenuated by carvacrol. (C) Representative images of DAPI staining and TUNEL assays used to analyze apoptotic cells (200×). (D) Apoptotic status was also determined using an Annexin V-FITC binding assay. (E) The rates of apoptosis. CAR, carvacrol. Mean±SD (n=3). $^{c}P<0.01$ *vs* control; $^{e}P<0.05$, $^{f}P<0.01$ *vs* the Fe^{2+}-treated group.

lated by Fe^{2+}. SH-SY5Y cells were treated with 10, 50, 100, 200 or 300 μmol/L of Fe^{2+} for 24 h and for 1, 3, 6, 12, or 24 h with 200 μmol/L Fe^{2+}, and then qPCR and Western blot analyses were used to determine the expression of NF-κB mRNA and protein. Both the mRNA and protein levels of NF-κB increased in concentration- and time-dependent manners after Fe^{2+} exposure (Figure 4). NF-κB mRNA levels increased significantly following the addition of 50 μmol/L Fe^{2+} and after 3-h Fe^{2+} exposure compared to control cells (Figure 4A and 4B). Similar behavior was observed for NF-κB protein expression levels, which increased significantly following the exposure to 100 μmol/L Fe^{2+} and after 6 h of exposure to Fe^{2+} compared to control cells (Figure 4C and 4D).

Carvacrol attenuates Fe^{2+}-induced NF-κB expression and translocation into the nucleus.

Cells were pretreated with carvacrol (333 μmol/L) for 2 h and then stimulated with Fe^{2+} (200 μmol/L) for 24 h. Western blot analysis was conducted to examine the effects of carvacrol on the Fe^{2+}-induced upregulation of NF-κB proteins in SH-SY5Y cells. The results indicated that carvacrol exhibited a significant inhibitory effect on the Fe^{2+}-induced increase in the expression of NF-κB (Figure 5A and 5B). We also showed that the nuclear translocation of NF-κB was significantly

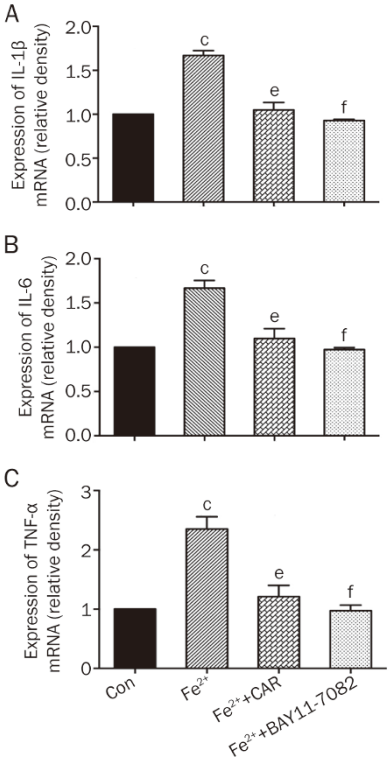

Figure 3. The effects of carvacrol on the expression of IL-1β (A), IL-6 (B) and TNF-α (C) in Fe^{2+}-stimulated SH-SY5Y cells. SH-SY5Y cells were pretreated with carvacrol (333 μmol/L) or BAY11-7082 (10 μmol/L) for 2 h and then exposed to Fe^{2+} (200 μmol/L) for 24 h. GAPDH was used as an internal control. CAR, carvacrol. Mean±SD (n=3). ^{c}P<0.01 *vs* the untreated control; ^{e}P<0.05, ^{f}P<0.01 *vs* the Fe^{2+}-treated group.

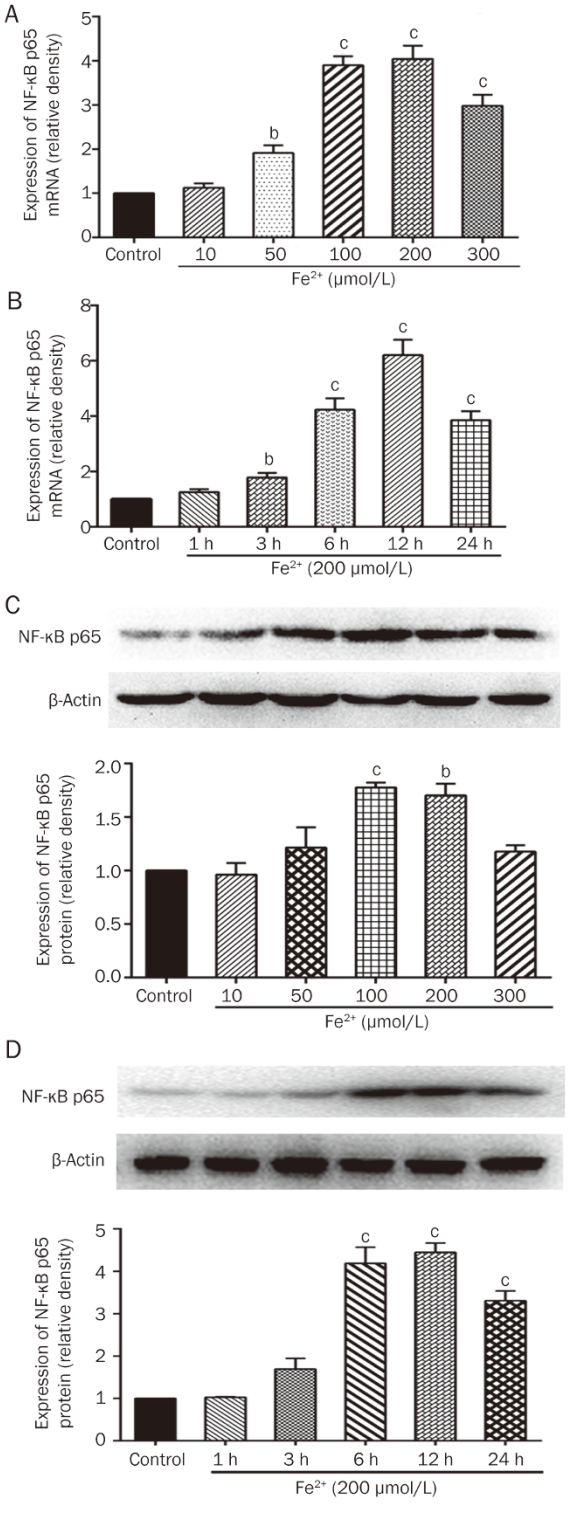

Figure 4. Effect of Fe^{2+} on the expression of NF-κB in SH-SY5Y cells. (A) The mRNA expression of NF-κB p65 in SH-SY5Y cells exposed to different concentrations of Fe^{2+} for 24 h. (B) The mRNA expression of NF-κB p65 in SH-SY5Y cells exposed to 200 μmol/L Fe^{2+} at different time-points. (C) Fe^{2+} increased the protein expression of NF-κB p65 in SH-SY5Y cells in a concentration-dependent manner. (D) Fe^{2+} increased the protein expression of NF-κB p65 in SH-SY5Y cells in a time-dependent manner. The data are presented as the mean±SD (n=3). ^{b}P<0.05 and ^{c}P<0.01, relative to the untreated control.

increased after 2 h of Fe^{2+}exposure. Immunofluorescence staining for intracellular NF-κB was examined by fluorescence confocal microscopy. In the control cell group, NF-κB was localized mainly in the cytosol. In SH-SY5Y cells treated with 200 μmol/L Fe^{2+} for 2 h, nuclear translocation of NF-κB was apparent. However, pre-incubation with carvacrol decreased Fe^{2+}-induced NF-κB translocation into the nucleus (Figure 5C). Nuclear and cytosolic extracts that were harvested from SH-SY5Y cells after treatment with Fe^{2+} with/without carvacrol were isolated, and the method used to isolate the cytosolic and nuclear fractions was validated using Western blot analysis (supplementary Figure S1). Exposure to Fe^{2+}at 200 μmol/L for 2 h significantly increased the nuclear translocation of NF-κB. Pre-incubation with carvacrol at 333 μmol/L for 2 h prior to treatment with Fe^{2+} significantly decreased the level of NF-κB protein that translocated into the nucleus (Figure 5D).

The activation of NF-κB is known to be mediated by a wide variety of upstream signals. Next, we tested the role of MAPKs in the processes involved in Fe^{2+}-induced NF-κB translocation in SH-SY5Ycells. Cells were pre-incubated with different MAPKs inhibitors (SB203580, U0126, and SP600125) or 333 μmol/L carvacrol for 2 h and then treated with 200 μmol/L Fe^{2+} for 2 h. Nuclear and cytosolic extracts were then harvested from SH-SY5Y cells. NF-κB p65 levels were measured using Western blot analysis. The results indicated that both carvacrol and JNK inhibitor, SP600125, inhibited NF-κB translocation in Fe^{2+}-stimulated SH-SY5Y cells, while ERK and p38 inhibitors did not (Figure 6A).

Carvacrol protects against Fe^{2+}-induced cell apoptosis by inactivating the MAPK/JNK-NF-κB pathway

Cells were pretreated with carvacrol (333 μmol/L) for 2 h and then stimulated with Fe^{2+} (200 μmol/L) for 2 h. Western blot analysis was conducted to examine the effects of carvacrol on the activation of IKK and MAPKs in SH-SY5Y cells. As shown in Figure 6B and 6C, cells exposed to Fe^{2+} induced p38, ERK, JNK, and IKK phosphorylation, and pretreatment with carvacrol inhibited Fe^{2+}-induced JNK and IKK phosphorylation but had no apparent effect on ERK and p38 phosphorylation .

Based on this evidence, we next investigated the possible roles of SP600125 and BAY11-7082 (inhibitors of MAPK/JNK and NF-κB, respectively) in apoptotic cell death induced by Fe^{2+}. The results demonstrated that pretreatment with BAY11-7082 and SP600125 (10 μmol/L) for 2 h markedly inhibited the increase in caspase-3 protein expression in SH-SY5Y cells (Figure 7). Therefore, all of the results indicate that carvacrol protects SH-SY5Y cells against apoptotic cell death and that these protective effects might be related to the inhibition of MAPK/JNK and IKK activation and the subsequently decreased activation of NF-κB.

Discussion

In the present study, we demonstrated that carvacrol was able to inhibit Fe^{2+}-induced neurotoxicity in a dose-dependent manner in SH-SY5Y cells. The underlying mechanisms involved in this process were associated with reducing Fe^{2+}-

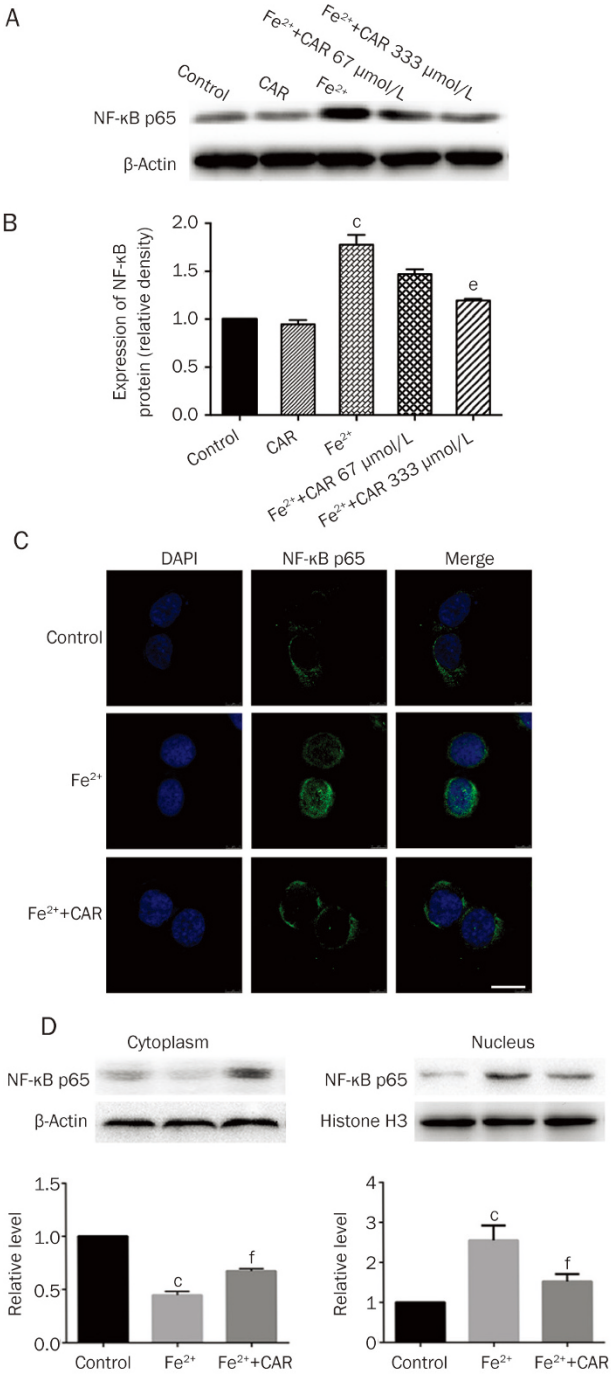

Figure 5. Effects of carvacrol on the Fe^{2+}-induced activation of NF-κB in SH-SY5Y cells. (A) Carvacrol (333 μmol/L) had a significant inhibitory effect on the Fe^{2+}-induced increase in the expression of NF-κB p65 compared to the Fe^{2+}-treated group. (B) Carvacrol-induced reduction in the protein level of NF-κB p65. (C) NF-κB nuclear translocation was analyzed using a confocal microscope, which showed that NF-κB p65 was translocated to the nucleus from the cytosol after Fe^{2+} treatment. Carvacrol abolished Fe^{2+}-induced NF-κB translocation into the nucleus. Scale bar=20 μm. (D) NF-κB p65 expression in the cytoplasm and nuclei was measured using Western blot analysis. Bar graph illustrating the relative protein level compared with the control. CAR, carvacrol. The data are presented as the mean±SD (n=3). ^{c}P<0.01, *vs* untreated control; ^{e}P<0.05, ^{f}P<0.01, *vs* Fe^{2+}-treated group.

induced neurotoxicity, which was mediated by the attenuation of apoptosis through the downregulation the MAPK/JNK-NF-κB signaling pathway.

Fe^{2+}, a hemoglobin degradation product, plays a key role in neurodegeneration in many disease states. Evidence indicates that Fe^{2+} overload also contributes to brain injury after intracerebral hemorrhage[36]. A large amount of Fe^{2+} is released by dying erythrocytes after hemorrhagic stroke. An excess increase of Fe^{2+} in the brain has been shown to be accompanied by a corresponding elevation in reactive oxygen species production and a higher susceptibility to neuronal cell death. In this study, we explored the cytotoxicity of Fe^{2+} in SH-SY5Y cells using CCK-8 assays. The results demonstrated that Fe^{2+} decreased cell viability in a dose-dependent manner. We found that Fe^{2+} treatment at 200 μmol/L for 24 h greatly decreased cell viability. However, pretreatment with different concentrations of carvacrol markedly attenuated this reduction in cell viability. There is evidence showing that Fe^{2+}-induced neurotoxicity occurs via the activation of apoptotic pathways[37, 38]. The intrinsic apoptotic pathway is mainly regulated by proteins that belong to the Bcl-2 and caspase families. It has been suggested that the increase in ROS formation that is induced by Fe^{2+} leads to cellular apoptosis through the accumulation of Bax and the activation of caspase-3[17, 39]. Therefore, the inhibition of pro-apoptotic Bax expression or caspase-3 activity and the upregulation of anti-apoptotic Bcl-2 expression may be associated with neuroprotective effects against Fe^{2+}. Consistent with these results, in this study, Fe^{2+} treatment caused an increase in the Bax/Bcl-2 ratio and an elevation in caspase-3 activity in SH-SY5Y cells. This effect, however, was significantly attenuated by carvacrol, suggesting that carvacrol effectively protects SH-SY5Y cells against Fe^{2+}-induced cytotoxicity by regulating apoptosis.

It has been suggested that inflammation is involved in neuronal death and that a wide range of pro-inflammatory factors, such as TNF-α, IL-1β and IL-6, might be toxic to neurons[40]. In addition, ROS may initiate and exaggerate inflammatory responses through their involvement in specific signaling path-

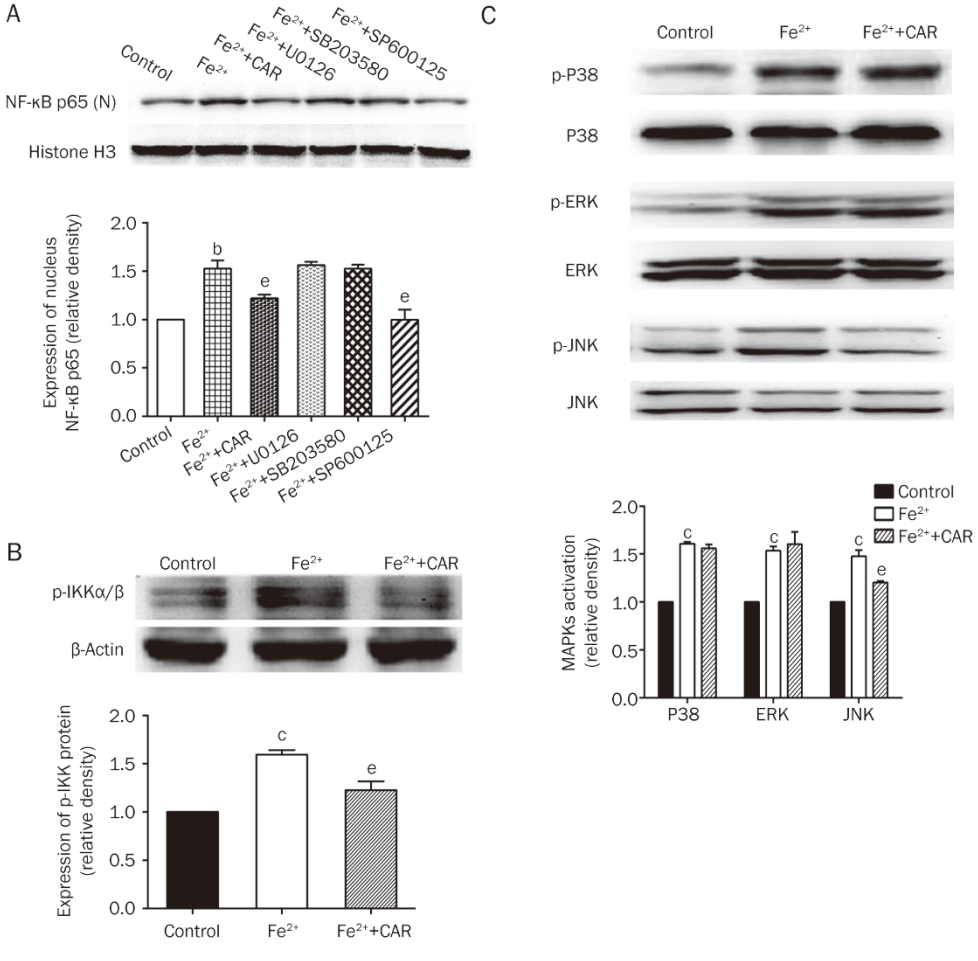

Figure 6. MAPKs were involved in the activation of NF-κB p65 in Fe^{2+}-stimulated SH-SY5Y cells. (A) Both carvacrol and JNK inhibitor, SP600125, inhibited NF-κB p65 translocation in Fe^{2+}-stimulated SH-SY5Y cells, while ERK and p38 inhibitors did not. (B) Fe^{2+} induced IKK phosphorylation in SH-SY5Y cells. Pretreatment with carvacrol inhibited Fe^{2+}-induced IKK phosphorylation. (C) Fe^{2+} induced p38, ERK, and JNK phosphorylation in SH-SY5Y cells. Pretreatment with carvacrol inhibited Fe^{2+}-induced JNK phosphorylation. Bar graph illustrating the relative protein level compared with the control. CAR, carvacrol, N=Nuclear. Mean±SD (n=3). $^{b}P<0.05$, $^{c}P<0.01$ *vs* the untreated control; $^{e}P<0.05$ *vs* the Fe^{2+}-treated group.

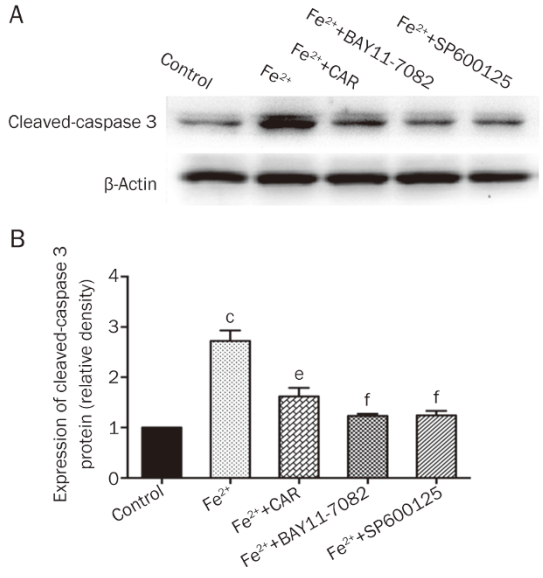

Figure 7. The neuroprotection provided by carvacrol-mediated inhibition of Fe^{2+}-induced caspase-3 expression is mediated by JNK/MAPK and NF-κB inactivation in SH-SY5Y cells. (A) Exposure to Fe^{2+} at 200 μmol/L for 24 h significantly increased caspase-3 protein levels, while pretreatment with carvacrol (333 μmol/L) for 2 h significantly downregulated the elevated protein expression level of caspase-3. Similarly, pretreatment with BAY11-7082 or SP600125 (10 μmol/L) for 2 h also markedly inhibited the increase in caspase-3 protein expression in SH-SY5Y cells. (B) The densities of the corresponding bands were measured, and the ratios were calculated. Mean±SD (n=3). CAR, carvacrol; ^{c}P<0.01 *vs* the untreated control; ^{e}P<0.05, ^{f}P<0.01 *vs* the Fe^{2+}-treated group.

ways, such as the NF-κB pathway[41, 42]. Activation of NF-κB has been implicated as an important pathway in the regulation of many genes that are involved in inflammatory responses, such as cytotoxic cytokines (IL-1β, IL-6 and TNF-α), resulting in the elevation of their expression in tissues and exerting direct cytotoxic effects[13]. Thus, it is of particular interest to determine whether the toxicity associated with Fe^{2+} is involved in the regulation of cytokine gene expression and whether this regulation is associated with the activation of the transcription factor NF-κB. In the present study, we found that exposing SH-SY5Y cells to Fe^{2+} resulted in elevated mRNA levels of the cytokines TNF-α, IL-1β and IL-6 and that pretreatment with carvacrol reversed the Fe^{2+}-induced increase in IL-1β, IL-6 and TNF-α expression in SH-SY5Y cells. A similar result was found when we used an inhibitor of NF-κB. Our results suggest that carvacrol confers neuroprotective effects and is able to inhibit proinflammatory mediators and that these anti-inflammatory effects might be involved in preventing the neuronal cell death caused by Fe^{2+}.

NF-κB is a pleiotropic transcription factor that plays an important role in the induction of pro-inflammation gene expression and is believed to be a promising new target for the treatment of inflammation and neuronal apoptosis[13, 35]. Normally, the inactive form of NF-κB is present in the cytoplasm as a heterodimer consisting of p50 and p65 subunits bound to an inhibitory IKb monomer[43]. Activation of IKKα/β, which is an upstream activator of NF-κB, by a variety of stimulators caused IKb phosphorylation, which promoted NF-κB release from the inhibitory subunit IKb in the cytoplasmic complex and the translocation of the DNA binding subunits to the nucleus, where they bind to specific DNA sequences, thereby enhancing the expression of many genes, including IL-1β, IL-6 and TNF-α[43-45]. In this study, the increased level of NF-κB is consistent with and is associated with the upregulation of IL-1β, IL-6 and TNF-α. Fe^{2+} not only increased the expression of NF-κB in a time- and concentration-dependent manner but also induced NF-κB translocation into the nucleus. This result suggests that NF-κB activation may play a pivotal role in Fe^{2+}-induced neuronal cell death. In addition, carvacrol exhibited a statistically inhibitory effect on the increased expression of NF-κB and also attenuated Fe^{2+}-induced NF-κB translocation from the cytoplasm to the nucleus when examined by Western blot analysis and immunocytochemistry.

It is now generally accepted that NF-κB plays dual roles in cell apoptosis[45]. In other studies, NF-κB activation has been shown to be either pro-apoptotic[14, 15, 35] or anti-apoptotic[45, 46], depending on the conditions and the cell types under investigation. In addition, in a cerebral ischemia study, the researchers found that the transient activation of NF-κB might be neuroprotective, while more persistent activation could be responsible for the induction of proteins that lead to neuronal cell death[47]. In the current study, our results show that the expression of NF-κB was significantly increased by treating SH-SY5Y cells with Fe^{2+}. We further studied whether the inhibition of NF-κB activation and translocation to the nucleus is also implicated in the mechanism of carvacrol antagonism of Fe^{2+}-induced apoptosis. Pretreatment with carvacrol significantly downregulated the elevated protein expression level of caspase-3, and pretreatment with BAY11-7082 also markedly inhibited the increase in caspase-3 protein expression in SH-SY5Y cells. These results suggest that NF-κB activation may play a critical role in Fe^{2+}-induced cell death. Carvacrol provided neuroprotection by inhibiting the activation of NF-κB by Fe^{2+} and subsequently decreased the production of pro-inflammatory cytokines.

Moreover, it has been suggested that ROS, which are induced by Fe^{2+}, are intracellular messengers that modulate diverse downstream signaling molecules, including NF-κB and MAPKs[43, 48], both of which might be downstream targets of ROS signaling pathways. The activation of these genes could result in the induction of inflammatory genes. In this study, carvacrol suppressed Fe^{2+}-induced NF-κB translocation to the nucleus and inhibited the activation of MAPKs and IKK. These results suggest that carvacrol-mediated attenuation of cell apoptosis is associated with the inhibition of NF-κB and MAPKs. Several studies have also shown that MAPKs are upstream activators of NF-κB and that the activation of JNK pathways is associated with neuronal death in both Parkinson disease and Alzheimer's disease[15, 19, 21, 35]. This idea is supported by our study, in which JNK inhibitors inhibited Fe^{2+} induced NF-κB activation and caspase-3 activityin SH-SY5Y

cells, while ERK and p38 inhibitors did not. As shown in Figure 6C, carvacrol was able to block the activation of the JNK pathways that were induced by Fe^{2+}, but it did not block the ERK or p38 MAPK pathways.

All of these results suggest that carvacrol may exert its neuroprotective effects against Fe^{2+}-induced cytotoxicity by inhibiting JNK and NF-κB activation, which consequently suppresses inflammatory factors. However, there is evidence demonstrating that in addition to its anti-inflammatory properties, carvacrol may also decrease the level of ROS production. In addition, an increase in the formation of ROS may initiate and exaggerate inflammatory responses through their ability to activate diverse signaling pathways that regulate inflammatory signaling cascades. This idea was confirmed by our follow-up studies (supplementary Figure S2). We found that incubation of SH-SY5Y cell with Fe^{2+} significantly increased ROS production and that this increase could be attenuated by carvacrol. Thus, whether the neuroprotective effects provided by carvacrol against Fe^{2+}-induced cytotoxicity act through the inhibition of JNK and NF-κB activation directly or through the prevention of ROS formation requires further investigation (Figure 8).

Conclusions

In summary, our results show that exposure to Fe^{2+} upregulates IL-1β, IL-6 and TNF-α mRNA expression in SH-SY5Y cells. This suggests that they may contribute to the initiation of apoptosis. We demonstrated that carvacrol inhibits Fe^{2+}-induced neurotoxicity by downregulating a signaling pathway that involves MAPK/JNK signaling and by reducing NF-κB-mediated proinflammatory factors in the SH-SY5Y cell line.

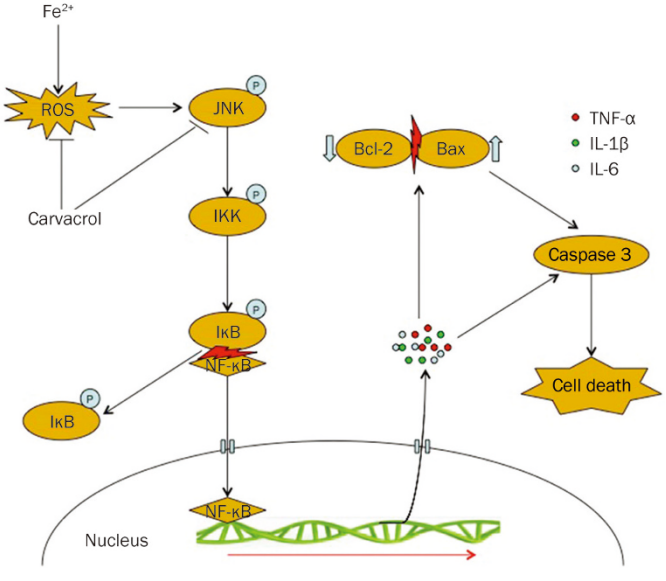

Figure 8. Schematic representation of the proposed mechanisms of carvacrol cytoprotection against Fe^{2+}-induced apoptosis. Fe^{2+}stimulates mitochondrial ROS generation and MAPK/JNK and IKK phosphorylation, which may promote NF-κB activation and nuclear translocation. Increased nuclear binding of NF-κB induces the increased expression of pro-inflammatory factors (IL-1β, IL-6 and TNF-α), which activate downstream apoptotic signaling pathways, ultimately resulting in cell death. Carvacrol reduces Fe^{2+}-induced cell apoptosis by inactivating the MAPK/JNK-NF-κB signaling pathway.

Acknowledgements

This research was supported by a SJTU Medicine-Engineering Research Fund (Grant No YG2012MS06 and YG2014QN17) and grants from the National Natural Science Foundation of China (81471176 and 81301045).

Author contribution

Liu-guan BIAN and Zhen-wen CUI participated in designing the study and preparing the manuscript; Zhen-wen CUI, Zheng-xing XIE, Bao-feng WANG, and Zhi-hong ZHONG performed the experiments; Zhen-wen CUI, Zheng-xing XIE, Xiao-yan CHEN, Yu-hao SUN, Qing-fang SUN, and Guo-yuan YANG analyzed the data; and Liu-guan BIAN was responsible for supervision and funding. All authors read and approved the final version of the manuscript.

Supplementary information

Supplementary information is available at Acta Pharmacologica Sinica's website.

References

1 Minhas G, Modgil S, Anand A. Role of iron in ischemia-induced neurodegeneration: mechanisms and insights. Metab Brain Dis 2014; 29: 583–91.
2 Loftspring MC, Hansen C, Clark JF. A novel brain injury mechanism after intracerebral hemorrhage: the interaction between heme products and the immune system. Med Hypotheses 2010; 74: 63–6.
3 Zhu X, Raina AK, Lee HG, Casadesus G, Smith MA, Perry G. Oxidative stress signalling in Alzheimer's disease. Brain Res 2004; 1000: 32–9.
4 Berg D, Gerlach M, Youdim MB, Double KL, Zecca L, Riederer P, *et al.* Brain iron pathways and their relevance to Parkinson's disease. J Neurochem 2001; 79: 225–36.
5 Pelizzoni I, Macco R, Morini MF, Zacchetti D, Grohovaz F, Codazzi F. Iron handling in hippocampal neurons: activity-dependent iron entry and mitochondria-mediated neurotoxicity. Aging Cell 2011; 10: 172–83.
6 Crichton RR, Wilmet S, Legssyer R, Ward RJ. Molecular and cellular mechanisms of iron homeostasis and toxicity in mammalian cells. J Inorg Biochem 2002; 91: 9–18.
7 Salvador GA, Oteiza PI. Iron overload triggers redox-sensitive signals in human IMR-32 neuroblastoma cells. Neurotoxicology 2011; 32: 75–82.
8 Wilson MR, Lightbody JH, Donaldson K, Sales J, Stone V. Interactions between ultrafine particles and transition metals *in vivo* and *in vitro*. Toxicol Appl Pharmacol 2002; 184: 172–9.
9 Kim EJ, Kwon KJ, Park JY, Lee SH, Moon CH, Baik EJ. Neuroprotective effects of prostaglandin E2 or cAMP against microglial and neuronal free radical mediated toxicity associated with inflammation. J Neurosci Res 2002; 70: 97–107.
10 Smith CJ, Lawrence CB, Rodriguez-Grande B, Kovacs KJ, Pradillo JM, Denes A. The immune system in stroke: clinical challenges and their translation to experimental research. J Neuroimmune Pharmacol 2013; 8: 867–87.
11 Mracsko E, Veltkamp R. Neuroinflammation after intracerebral hemorrhage. Front Cell Neurosci 2014; 8: 388.

12 Zhou Y, Wang Y, Wang J, Anne Stetler R, Yang QW. Inflammation in intracerebral hemorrhage: from mechanisms to clinical translation. Prog Neurobiol 2014; 115: 25–44.
13 Barnes PJ, Karin M. Nuclear factor-kappaB: a pivotal transcription factor in chronic inflammatory diseases. N Engl J Med 1997; 336: 1066–71.
14 Hickenbottom SL, Grotta JC, Strong R, Denner LA, Aronowski J. Nuclear factor-kappaB and cell death after experimental intracerebral hemorrhage in rats. Stroke 1999; 30: 2472–7.
15 Xing B, Liu M, Bing G. Neuroprotection with pioglitazone against LPS insult on dopaminergic neurons may be associated with its inhibition of NF-kappaB and JNK activation and suppression of COX-2 activity. J Neuroimmunol 2007; 192: 89–98.
16 O'Neill LA, Kaltschmidt C. NF-kappa B: a crucial transcription factor for glial and neuronal cell function. Trends Neurosci 1997; 20: 252–8.
17 Kooncumchoo P, Sharma S, Porter J, Govitrapong P, Ebadi M. Coenzyme Q(10) provides neuroprotection in iron-induced apoptosis in dopaminergic neurons. J Mol Neurosci 2006; 28: 125–41.
18 Youdim MB, Grunblatt E, Mandel S. The pivotal role of iron in NF-kappa B activation and nigrostriatal dopaminergic neurodegeneration. Prospects for neuroprotection in Parkinson's disease with iron chelators. Ann N Y Acad Sci 1999; 890: 7–25.
19 Borsello T, Forloni G. JNK signalling: a possible target to prevent neurodegeneration. Curr Pharm Des 2007; 13: 1875–86.
20 Kuperstein F, Yavin E. Pro-apoptotic signaling in neuronal cells following iron and amyloid beta peptide neurotoxicity. J Neurochem 2003; 86: 114–25.
21 Xie Z, Smith CJ, Van Eldik LJ. Activated glia induce neuron death via MAP kinase signaling pathways involving JNK and p38. Glia 2004; 45: 170–9.
22 Baser KH. Biological and pharmacological activities of carvacrol and carvacrol bearing essential oils. Curr Pharm Des 2008; 14: 3106–19.
23 Nafees S, Ahmad ST, Arjumand W, Rashid S, Ali N, Sultana S. Carvacrol ameliorates thioacetamide-induced hepatotoxicity by abrogation of oxidative stress, inflammation, and apoptosis in liver of Wistar rats. Hum Exp Toxicol 2013; 32: 1292–304.
24 Guimaraes AG, Xavier MA, de Santana MT, Camargo EA, Santos CA, Brito FA, *et al.* Carvacrol attenuates mechanical hypernociception and inflammatory response. Naunyn Schmiedebergs Arch Pharmacol 2012; 385: 253–63.
25 Aeschbach R, Loliger J, Scott BC, Murcia A, Butler J, Halliwell B, *et al.* Antioxidant actions of thymol, carvacrol, 6-gingerol, zingerone and hydroxytyrosol. Food Chem Toxicol 1994; 32: 31–6.
26 Arigesavan K, Sudhandiran G. Carvacrol exhibits anti-oxidant and anti-inflammatory effects against 1, 2-dimethyl hydrazine plus dextran sodium sulfate induced inflammation associated carcinogenicity in the colon of Fischer 344 rats. Biochem Biophys Res Commun 2015; 461: 314–20.
27 Suo L, Kang K, Wang X, Cao Y, Zhao H, Sun X, *et al.* Carvacrol alleviates ischemia reperfusion injury by regulating the PI3K-Akt pathway in rats. PLoS One 2014; 9: e104043.
28 Canbek M, Uyanoglu M, Bayramoglu G, Senturk H, Erkasap N, Koken T, *et al.* Effects of carvacrol on defects of ischemia-reperfusion in the rat liver. Phytomedicine 2008; 15: 447–52.
29 Chen W, Xu B, Xiao A, Liu L, Fang X, Liu R, *et al.* TRPM7 inhibitor carvacrol protects brain from neonatal hypoxic-ischemic injury. Mol Brain 2015; 8: 11.
30 Yu W, Liu Q, Zhu S. Carvacrol protects against acute myocardial infarction of rats via anti-oxidative and anti-apoptotic pathways. Biol Pharm Bull 2013; 36: 579–84.
31 Landa P, Kokoska L, Pribylova M, Vanek T, Marsik P. *In vitro* anti-inflammatory activity of carvacrol: Inhibitory effect on COX-2 catalyzed prostaglandin E(2) biosynthesis. Arch Pharm Res 2009; 32: 75–8.
32 Kara M, Uslu S, Demirci F, Temel HE, Baydemir C. Supplemental Carvacrol Can Reduce the Severity of Inflammation by Influencing the Production of Mediators of Inflammation. Inflammation 2015; 38: 1020–7.
33 Lima Mda S, Quintans-Junior LJ, de Santana WA, Martins Kaneto C, Pereira Soares MB, Villarreal CF. Anti-inflammatory effects of carvacrol: evidence for a key role of interleukin-10. Eur J Pharmacol 2013; 699: 112–7.
34 Gholijani N, Gharagozloo M, Farjadian S, Amirghofran Z. Modulatory effects of thymol and carvacrol on inflammatory transcription factors in lipopolysaccharide-treated macrophages. J Immunotoxicol 2015: 1–8.
35 Yu Y, Zhou L, Sun M, Zhou T, Zhong K, Wang H, *et al.* Xylocoside G reduces amyloid-beta induced neurotoxicity by inhibiting NF-kappaB signaling pathway in neuronal cells. J Alzheimers Dis 2012; 30: 263–75.
36 Huang FP, Xi G, Keep RF, Hua Y, Nemoianu A, Hoff JT. Brain edema after experimental intracerebral hemorrhage: role of hemoglobin degradation products. J Neurosurg 2002; 96: 287–93.
37 Miwa CP, de Lima MN, Scalco F, Vedana G, Mattos R, Fernandez LL, *et al.* Neonatal iron treatment increases apoptotic markers in hippocampal and cortical areas of adult rats. Neurotox Res 2011; 19: 527–35.
38 Zhang Z, Wei T, Hou J, Li G, Yu S, Xin W. Iron-induced oxidative damage and apoptosis in cerebellar granule cells: attenuation by tetramethylpyrazine and ferulic acid. Eur J Pharmacol 2003; 467: 41–7.
39 Liu R, Liu W, Doctrow SR, Baudry M. Iron toxicity in organotypic cultures of hippocampal slices: role of reactive oxygen species. J Neurochem 2003; 85: 492–502.
40 Kim YS, Joh TH. Microglia, major player in the brain inflammation: their roles in the pathogenesis of Parkinson's disease. Exp Mol Med 2006; 38: 333–47.
41 Asehnoune K, Strassheim D, Mitra S, Kim JY, Abraham E. Involvement of reactive oxygen species in Toll-like receptor 4-dependent activation of NF-kappa B. J Immunol 2004; 172: 2522–9.
42 Wang T, Qin L, Liu B, Liu Y, Wilson B, Eling TE, *et al.* Role of reactive oxygen species in LPS-induced production of prostaglandin E2 in microglia. J Neurochem 2004; 88: 939–47.
43 Flohe L, Brigelius-Flohe R, Saliou C, Traber MG, Packer L. Redox regulation of NF-kappa B activation. Free Radic Biol Med 1997; 22: 1115–26.
44 Guo Z, Shao L, Du Q, Park KS, Geller DA. Identification of a classic cytokine-induced enhancer upstream in the human iNOS promoter. FASEB J 2007; 21: 535–42.
45 Kaltschmidt B, Widera D, Kaltschmidt C. Signaling via NF-kappaB in the nervous system. Biochim Biophys Acta 2005; 1745: 287–99.
46 Zhang J, Li Y, Yu M, Chen B, Shen B. Lineage-dependent NF-kappaB activation contributes to the resistance of human macrophages to apoptosis. Hematol J 2003; 4: 277–84.
47 Clemens JA, Stephenson DT, Yin T, Smalstig EB, Panetta JA, Little SP. Drug-induced neuroprotection from global ischemia is associated with prevention of persistent but not transient activation of nuclear factor-kappaB in rats. Stroke 1998; 29: 677–82.
48 Kim KK, Singh RK, Strongin RM, Moore RG, Brard L, Lange TS. Organometallic iron(III)-salophene exerts cytotoxic properties in neuroblastoma cells via MAPK activation and ROS generation. PLoS One 2011; 6: e19049.